# A review of physical flexible ship models used for hydroelastic experiments

Grammatikopoulos, Apostolos

**Citation (APA)**
Grammatikopoulos, A. (2023). A review of physical flexible ship models used for hydroelastic experiments. *Marine Structures*, *90*, Article 103436. https://doi.org/10.1016/j.marstruc.2023.103436
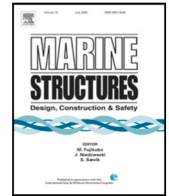
Review article

# A review of physical flexible ship models used for hydroelastic experiments

Apostolos Grammatikopoulos

*Maritime and Transport Technology, Delft University of Technology, Mekelweg 2, 2628 CD, Delft, The Netherlands*

## ARTICLE INFO

## ABSTRACT

Hydroelasticity of ships has been established as a necessary form of investigation for both slender ships and high-speed craft. Experimental investigations have spanned various topics, including symmetric and antisymmetric, harmonic and transient, linear and nonlinear responses. Models have varied in size and the way the structure is modelled, depending of the focus of the investigation. The multitude of interacting physical mechanisms introduce almost-impossible-to-resolve scaling issues, and the eventual compromises depend on the aim of the investigator. This publication provides a comprehensive review of the evolution of these experimental techniques, from the first appearances of the field to the modern state-of-the-art and potential future directions.

## 1. Introduction

Flexible structural models have been used extensively for the investigation of dynamic responses since the end of World War II [1,2]. Rigid ship models, used in towing tank tests, have an even longer history, beginning at the time of William Froude. Even though computational techniques were first established in the 1970s and have since progressed significantly, the concept of model experiments still constitutes an essential part of the scientific method. Using full-scale measurements would be, of course, the best approach to obtain realistic data, but it is expensive, time-consuming, and potentially dangerous for the crew, while the weather conditions are uncontrollable and not necessarily easy to measure [3]. Consequently, despite the uncertainties caused by scaling effects, physical models are often considered the most credible method of investigation and are used for validation of theoretical and numerical models.

In the case of experiments in the towing tank, the so-called Froude scaling is used. Froude scaling involves uniform scaling of all model and wave dimensions, thus satisfying geometric similarity. Any part of the structure that may come in contact with the water should be accurately scaled. It should be noted that "dimensions" may include any quantity measured in $L^n$, where $L$ stands for length units. For example, the longitudinal centre of gravity or the metacentric height would be scaled by $\lambda$, whereas the submerged volume of the vessel would then be equal to:

$$\nabla_M = \frac{\nabla_F}{\lambda^3} \tag{1}$$

where $\nabla_M, \nabla_F$ are the vessel displaced volumes at model and full scale, respectively. The mass can be consequently calculated as:

$$m_M = \frac{\rho_M}{\rho_F} \frac{m_F}{\lambda^3} \tag{2}$$

where $\rho_M, \rho_F$ is the density of water in model-scale and full-scale, respectively. This means that the mass is scaled in proportion to the cube of the similarity ratio only if water in the towing tank has the same density as the one surrounding the full-scale vessel.

*E-mail address:* A.Grammatikopoulos@tudelft.nl.

However, the $\rho_M/\rho_F$ ratio is approximately equal to unity and can be neglected when performing initial scaling estimations. It can be similarly proven that any second moment of area and mass moment of inertia are scaled in proportion to the fourth and the fifth power of the similarity ratio, respectively.

A constant Froude number between full-scale and model-scale vessel ensures not only kinematic but also dynamic similarity, as the ratio of inertia forces over gravity forces results in a correct scaling of gravity waves. Creating Froude-similar models means that velocity is scaled down in proportion to the square root of the similarity ratio. Although Reynolds similarity (i.e. ratio of inertia forces over viscous forces) would also be desirable, it can be easily proven that satisfying both relationships is impossible [4]. As viscous forces are relatively small in most cases of ship motions, Reynolds similarity is often abandoned and turbulence inducers are potentially used to initiate turbulence at a pre-calculated transition point instead.

The beam mathematical model is often used to simulate the behaviour of a ship, where the boundary conditions are selected as free for both ends. As a consequence, the normal stress in a cross-section when the ship is subjected to a combination of vertical bending and axial loads can be expressed as:

$$\sigma \propto \left( \frac{F_x}{A} + \frac{M_{yy}z}{I_{yy}} \right) \tag{3}$$

where $F_x$ and $A$ denote the axial force and cross-sectional area and $M_{yy}$, $z$ and $I_{yy}$ represent the vertical bending moment, distance from the neutral axis and second moment of area, respectively. As discussed earlier, distance scales linearly, area scales as $\lambda^2$, force scales as $\lambda^3$, and $M_{yy}$ and $I_{yy}$ scale as $\lambda^4$. Substituting into (3), we obtain:

$$\sigma_F = \lambda \sigma_M \tag{4}$$

In order to maintain geometric similarity, all displacements should scale accordingly. As a result, strains should be the same for the full-scale and model-scale ships. The normal stress can also be expressed as:

$$\sigma \propto E\epsilon \tag{5}$$

where $E$ is the modulus of elasticity and $\epsilon$ is the relevant strain. Combining (4) and (5) we obtain:

$$E_F = \lambda E_M \tag{6}$$

which means that the elastic modulus of the material used for the model should scale linearly as well.

As the above is very restrictive, complete similarity is rarely achieved in physical modelling and simplifications are often employed. When *first-order similarity* is used, some scaling laws are ignored as not relevant to the condition simulated. They may regard boundary conditions, geometry, or material used. The selection of pertinent scaling laws is based on the characterisation of the loading condition as axial, bending, shear, torsion, or any combination of the four [5].

Axial loads on a ship are also considered negligible compared to bending loads and a pure bending approximation can be assumed for symmetric loading. Consequently, scaling of the cross-sectional area becomes less important and scaling of the bending stiffness becomes, in turn, essential. Calculating the bending-induced strain:

$$\left( \frac{M_{yy}z}{EI_{yy}} \right)_F = \left( \frac{M_{yy}z}{EI_{yy}} \right)_M \tag{7}$$

which means that:

$$\left( EI_{yy} \right)_F = \lambda^5 \left( EI_{yy} \right)_M \tag{8}$$

For a uniform Euler beam [6], the $r^{th}$ natural frequency in vertical bending is calculated using:

$$\omega_r = \frac{(\kappa L)_r^2}{L^2} \sqrt{\frac{EI}{\mu}} \tag{9}$$

where $\mu$ is the mass per unit length, $L$ is the length of the vessel, and $(\kappa L)_r$ for a free–free beam are the solutions of:

$$\cosh \kappa L \cos \kappa L = 1 \tag{10}$$

For the full scale vessel, (9) becomes:

$$(\omega_r)_F = \frac{(\kappa L_M)_r^2}{\lambda^2 L_M^2} \sqrt{\frac{\lambda^5 (EI)_M}{\lambda^2 \mu_M}} \iff (\omega_r)_F = \lambda^{-\frac{1}{2}} (\omega_r)_M \tag{11}$$

which means that matching strains between model scale and full scale are a necessary and sufficient condition for appropriate scaling of the bending natural frequencies. Conversely, any discrepancy in the scaling of natural frequencies directly affects the accuracy of the measured strains.

Dependency of scaling of the dry natural frequencies only on the bending stiffness distribution (and mass distribution) means that the elastic modulus and second moment of area distribution do not need to be scaled separately. Based on this principle, the design process is greatly facilitated by depicting the stiffness in a simplified manner, often without the existence of a structural cross-section (flexible joint models).

(a) Flexible backbone model [7]



(b) Flexible joint model [8]



(c) Elastic model [3]
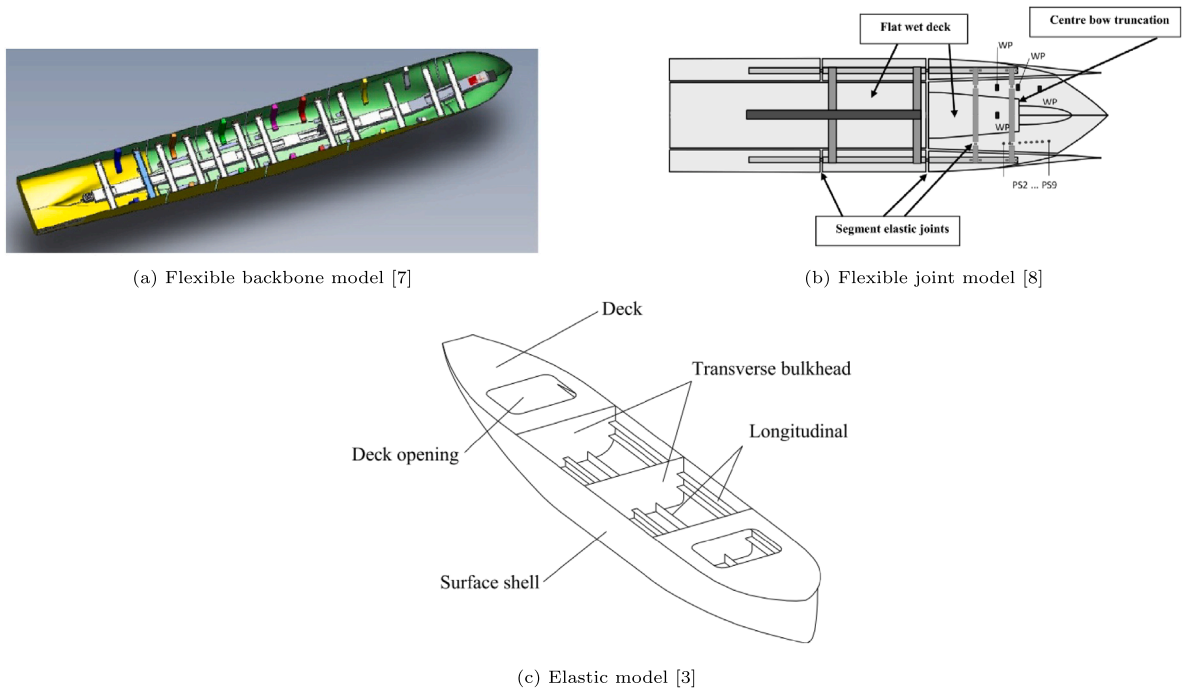
**Fig. 1.** Schematics of the three types of flexible models.

Although considering shear contributions (Timoshenko beam approximation) and warping contributions (Vlasov beam approximation) will, in most cases, affect the dynamic responses, precise scaling of the equivalent shear area and the warping constant of the cross section is very challenging to achieve and also less important. The largest difference in the responses arises from the move from infinite to finite values for these properties, and the variation based on the exact value is significantly smaller for symmetric responses. As will be discussed in Section 3, such discrepancies can be considered acceptable as long as their effects are measurable/quantifiable.

This publication is intended to be a comprehensive review of the flexible ship models that have been used, through the decades, for hydroelastic experiments. Only full ship models are discussed, so drop tests using wedges or ship sections are omitted. Rigid ship models for load measurement, where the model is segmented but joined with force transducers and has no flexibility, are discussed very briefly at points. Full-scale measurements are beyond the scope of this publication, and are only mentioned when compared to experimental results. Details about the findings of experiments are discussed, among others to illustrate the capabilities and restrictions of various model designs.

Following the introduction to the basic scaling background above, Section 2 provides an introduction to the categories of flexible ship models. These are grouped based on the nature of the stiffness source. Section 3 follows by explaining the process behind the selection of the basic properties of the model, including, among others, the material of the stiffness source and the number of segments. Subsequently, Section 4 reviews models that have been used in various types of hydroelastic investigations and discusses their special characteristics. This section is divided into a series of subsections, each focusing on a different type of investigation. Subsequently, Section 5 revisits selected publications from the previous section to discuss the measurement and conversion techniques used for different types of models. Finally, the findings are summarised in Section 6. A summary of all the models discussed within this publication is also provided in Table 2.

## 2. Hydroelastic ship model categories

Ship models for hydroelastic experiments should be capable of realistically deforming under fluid excitation. Since uniform scaling is used for both model and environment, realistic deformations involve identical strains in model-scale and full-scale. Flexibility is achieved by either constructing a so-called elastic model or, more easily, by producing the model in rigid segments. In the latter case, the segments are joined by means of either a flexible backbone or a series of flexible joints (Fig. 1).

*Flexible backbone models* are the most common. The backbone is usually made of aluminium or steel and can have a uniform or non-uniform cross section along its length. Use of variable cross section allows for non-uniform bending stiffness distribution and, consequently, accurate scaling of more natural frequencies and mode shapes. Openings are sometimes created on the beam for antisymmetric vibration experiments. This approach emulates deck openings on the actual ship and aims to approximate the shear centre location and torsional stiffness distribution. This can be quite challenging as the shear centre for full scale container

ships is located significantly below keel level. Model deflection is measured by strain gauges along the backbone. In the case of antisymmetric vibrations, shear strains are measured using shear strain gauges along the backbone.

*Flexible joint models* are also relatively popular because of the inherently adjustable nature of the joints. The same set of joints can be used to emulate various stiffness levels and uniform or distributed stiffness [7]. They are, consequently, more easily adapted than backbone models and deformations are measured by sensors integrated with the joints (e.g. torsional springs [8]). Despite this advantage, flexible joint models are less popular than backbone models, as the lack of a continuous structure deprives the model of the effects of cross-sectional characteristics, as described above (e.g. effective shear area, location of shear centre).

*Elastic models* are the most complicated to design and produce, as the roles of hydrodynamic boundary and excited structure are not separated and the model hull should act concurrently as both. These models allow the measurements of strains anywhere on the hull using strain gauges. As always, lengths corresponding to the external geometry of the hull scale linearly (scaling factor $\lambda$). However, the bending stiffness should be decreased in proportion to $\lambda^5$ and can only be adjusted by modifying wall thickness and internal structural arrangement. The material used should be capable of generating the complex hull geometry while providing an elastic modulus resulting in the required stiffness. The structure should, of course, be manufactured to be watertight and the internal structure should ideally resemble the full-scale ship. If the latter is not true, the shear flow within the cross section can change significantly, resulting in a different effective shear area and, more importantly, torsional constant and location of shear centre.

It can be easily deduced that the above criteria limit the range of applicable materials and manufacturing methods significantly. Furthermore, similarity of the internal structure is often restricted to essential features, such as deck openings and bulkheads [9] to satisfy the necessary requirements for a realistic response. Combined with the fact that, unlike their segmented counterparts, elastic models cannot be modified after production, very few vessels of this type have been manufactured (e.g. [10–12]). All of the above models consisted of an external shell with a deck and transverse bulkheads, missing the cellular structure of a container ship. An improved, so-called *fully elastic* model, including significant detail in the internal structure, was produced by Grammatikopoulos et al. using additive manufacturing [13]. This method could potentially be used more extensively to produce geometrically accurate models with a limited manufacturing cost.

## 3. Selection of material, structural properties, and number of segments

The design principles for structural models, as the ones traditionally used, for example, by civil engineers, can differ from the ones related to hydroelastic models. The reason is that, for experiments where the excitation does not result from fluid–structure interaction, several design problems are eliminated (e.g. watertight structure, scaling of flow behaviour, etc.). Scaling law implementation is thus greatly facilitated, as it mainly involves geometric scaling and segmented models are not necessary — the resultant structure is usually continuous. If the material used to construct the model is different than the one in the full-scale structure, an additional scaling ratio is used for material similarity. The elastic models used in hydroelastic experiments can be considered a special case of these structural models, inheriting a large part of the relevant design methodology.

After the natural frequency similarity is established, the stress–strain curves of the material used should be carefully examined in conjunction with the estimated loads. It should be ensured that responses remain within the elastic region. Linear elastic behaviour is necessary for the principle of superposition to be applicable; hence, results measured in regular waves can be used to derive general conclusions only if the above condition is satisfied. When the elastic deformation limit of the material is exceeded, material similarity should be satisfied instead. The stress–strain curves of the full scale structure and the scaled model should have qualitatively the same form. The strain hardening phenomena, present in plastic response regions, should depict the scaled behaviour of the structure appropriately.

The Poisson's ratio of the two materials should be similar, especially if large deformations are expected. Ships' sizing means that they should normally be modelled as Timoshenko or Vlasov beams, for which shear effects are significant. Structural damping should also be similar when dynamic responses are investigated. However, scaling of these properties is often very difficult. The question arising is whether the experiments can be considered reliable in such cases. Going one step further from first-order similarity (as described in the introduction), the term *distorted models* refers to occasions where parameters pertinent to the experiment are improperly scaled. This practice is only suggested when the effects of the violation can be measured and their consequences identified. Poisson's ratios for most materials are known and can also be measured experimentally. Although there are several semi-empirical methods for estimation of structural damping, the phenomenon is not entirely understood and experimental determination through modal testing [14] is regarded as the most reliable method.

The number of segments of a model plays an equally crucial role. As the rigid segments will always remain "linear" in shape, segmentation of a model attempts to approximate the mode shape by something similar to a polyline. Mode shapes corresponding to higher natural frequencies have more nodes, which means the necessary number of segments increases with the number of modes that are expected to be excited. Wu et al. demonstrated this issue for the 2-node bending mode shape (Fig. 2), although the effect would be even more pronounced for mode shapes with more nodes.

A summary of all the models used in the investigations reviewed can be found in Table 2. Although the table does not cover the full details of the experiments, some trends are easily identified. For example, the fact that many researchers tend to reuse a model as many times as possible to compensate for the expensive nature of the production process [15–17]. Furthermore, the increased number of models produced as years progressed (accompanied by an increase in publications overall) demonstrates a rising interest in the field of hydroelasticity. A more detailed investigation of the trends in design selections reveals important aspects of the nature of hydroelastic experiments.
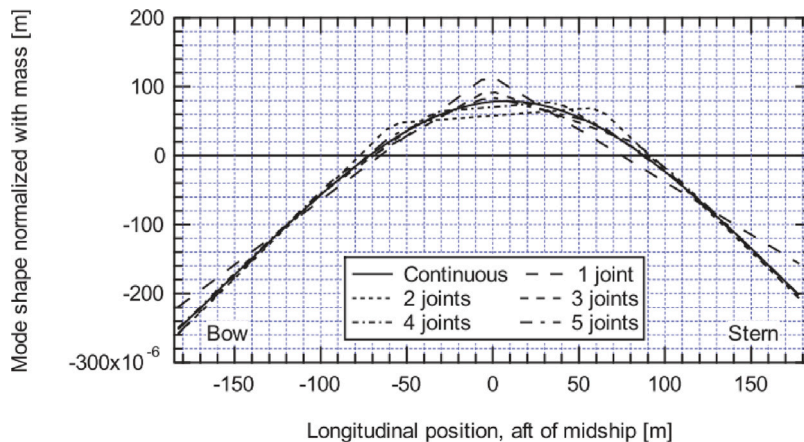
**Fig. 2.** Effect of segmentation on the approximation of the 2-node bending mode shape [7].

The way the ship's stiffness is modelled is one of the most essential aspects of the design process and it is used to categorise models. As mentioned earlier, the stiffness can result from the use of a flexible backbone, a series of flexible joints, or the vessel can be a continuous elastic model. As one might guess intuitively, the production cost and the related difficulty associated with elastic models results in them being a very rare choice. In fact, the number of elastic models documented in the literature corresponds to less than 15% of flexible models and was more popular in earlier years (see [10,11,18,19]). The use of a flexible backbone is, undoubtedly, the most popular, although flexible joints are also commonly used for specific types of investigations (e.g. [16,20–23]). Differences between these arrangements are discussed in more detail in Section 2.

Whilst the distribution of the stiffness in an elastic model is by default variable, uniform stiffness distribution is more commonly used for other model types. It has been demonstrated repeatedly (e.g in [24]) that the first natural frequency in vertical bending and the relevant responses can be accurately depicted without the complicated processes involved in accurate stiffness distribution modelling. Variable stiffness distribution was employed in cases where either more mode shapes became important [15] or torsional responses were investigated [25].

It can be observed from the data summary in Table 2 that the majority of researchers select a number of segments between 3 and 6. Slightly larger or smaller values are less common but researchers have applied them in the past for investigations with more specific aims. For example, 2-segment models are quite common in cases where the experiments focused on the loads amidships and the modal responses were not important [21,23,26]. More segments were used, in some cases, in hope of depicting the vessel modes more accurately [24,27–29]. Extreme cases include the elastic models, were there is no segmentation at all and few cases with very large number of segments [30,31]. The advantages of the latter have not been clearly demonstrated.

Structural damping can also play a detrimental role in the dynamic responses of models. It not only affects the amplitude of vibration, particularly around the region of resonance, but also the time after which transient responses die out. Table 2 summarises the modal damping ratio for the first dry mode (2-node bending). When only damping in water was mentioned, that was included instead, with a note in brackets. Damping in water includes, of course, contributions from viscous and radiation damping as well, which renders it less comparable to the remaining values.

It is interesting to observe that, despite the significance of this property, there is no available data for more than half of the models. Where available, most ratios range between approximately 0.5% and 2.0%. There is some evidence from full-scale measurements that this is the correct range for this property [32]. For segmented models, a big proportion of the damping originates from the elastic bands that are used to seal the gaps between segments and ensure the structure is watertight, which can also add stiffness for some modes [33]. For elastic models, damping is produced directly from the structure, and was found to be extremely high for older models [10,11] than newer ones [12]. Additive manufacturing using rigid plastic seems particularly promising, as it achieved even lower damping ratios than some segmented models [34].

## 4. Review of physical models used in hydroelastic experiments

Hydroelastic testing can vary not only in the way the model is designed and manufactured (as discussed in the previous section), but also the testing conditions and, as a result, the phenomena of interest. In Section 4.1, models that include stiffness not only longitudinally but also in the transverse direction are presented. In Section 4.2, benchmarking studies and uncommon experimental techniques will be discussed. In terms of testing conditions, it is clear that most of the data in the literature regards head waves and vertical bending (symmetric) responses. For example, Section 4.3 discusses slamming and whipping responses, Section 4.5 discusses nonlinear symmetric responses and Section 4.6 discusses use of symmetric response data to assess fatigue and buckling. Antisymmetric responses are treated separately in Section 4.4.
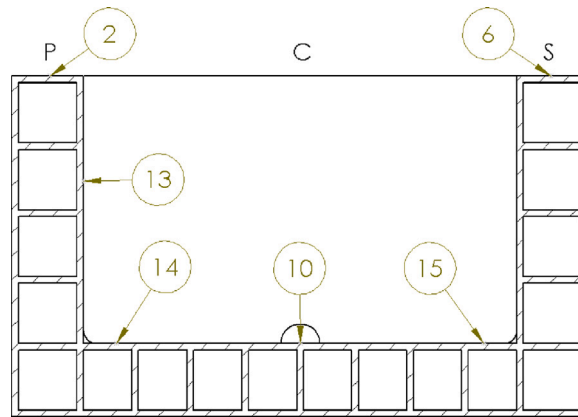
**Fig. 3.** The cross section of this elastic container ship model features a cellular structure. Strain gauges were installed throughout to obtain strain distributions within the cross section (shown with numbers) [13].

### 4.1. Models with multi-directional stiffness

As previously mentioned, the majority of flexible models use either a flexible backbone or flexible joints for segments along the length of the vessel. This section will present less common model designs, which attempt to include non-longitudinal components of stiffness. This includes both elastic models and models with other transverse stiffness sources.

Akita & Ochi created a 6-meter-long elastic model of a ship made out of brass, to measure motions and deflections [18]. The hull was of a generic ship shape and there are no indications that the structural properties represented those of a full-scale ship in any manner. Their investigation focused on responses in the wave–ship matching region, and also on slamming and the associated pressures and strains. Based on the experiments, they defined an "effective wave height ratio" as a metric to evaluate the slamming-induced stresses. More parametric studies were published in separate reports [35–37].

Fukasawa et al. produced an elastic model of a container ship using PVC foam [19]. The model consisted of an external shell and bulkheads, with the added detail of a near-cellular structure in the double bottom. It was self-propelled and subjected to head waves to investigate whipping responses. The authors argued that the high damping properties of the foam facilitated the identification of transient responses in the strain measurements, as it ensured that each whipping response was reduced to zero before the next slam occurred.

Chen et al. constructed an elastic model of the S-175 container ship using ABS [11]. The flexible material allowed them to use a sufficiently large scaling factor. However, the model comprised of only the outer shell and a number of transverse bulkheads — further detail in the internal structure would produce an excessively stiff model. The model design process is discussed more extensively in [9].

Houtani et al. manufactured an elastic model of a container ship out of urethane foam [38]. Once more, the model consisted of an external shell with large deck openings and a series of transverse bulkheads. The strain gauges installed on the hull were calibrated statically for vertical bending and torsion. The vessel was tested in an ocean basin, allowing the investigation of both symmetric and antisymmetric responses. The authors argued that segmented models, regardless of the backbone complexity and correct scaling of the first few natural frequencies (both symmetric and antisymmetric), cannot depict the behaviour of the full-scale ship. The above is a result primarily of the incorrect location of the shear centre, which should be below the keel, resulting in strong coupling between horizontal bending and torsion and can cause differences in the antisymmetric mode shapes between model- and full-scale vessel. A limitation of this design was that the material was more flexible than the strain gauges, which necessitated adjustment of the measured strains [12].

Grammatikopoulos et al. developed a design methodology to produce the so-called fully elastic models using additive manufacturing and ABS. This term was used to describe elastic models that do not only comprise of an external shell and bulkheads, but include more geometric detail internally. The authors demonstrated the need to test additively manufactured specimens and subject them to vibratory testing to predict the natural frequencies of a vessel manufactured in the same way [39]. This was necessitated by the fact that the dynamic and static flexural moduli of additively manufactured plastic models were found to be significantly different [34]. Despite externally looking like a rectangular barge, their model internally featured not only transverse bulkheads but also the cellular structure of a container ship (Fig. 3). Strain gauges were installed throughout the vessel and were calibrated by performing static tests on the entire model. Due to the aforementioned discrepancies between static and dynamic moduli, it can be argued that there is room for improvement regarding sensor calibration to reduce experimental uncertainty. The model was tested in regular head seas and linear and nonlinear springing responses were measured [13,40]. Testing in oblique waves demonstrated the capability of such a model to capture antisymmetric responses [13]. However, the model was significantly stiffer than intended, due to manufacturing limitations.

Tang et al. investigated the hydroelastic responses of a trimaran, using a 7-segment flexible backbone model [42]. The side hulls of the trimaran only had 2 segments each, with the aft-most cut coinciding for all three hulls. A primary backbone was used
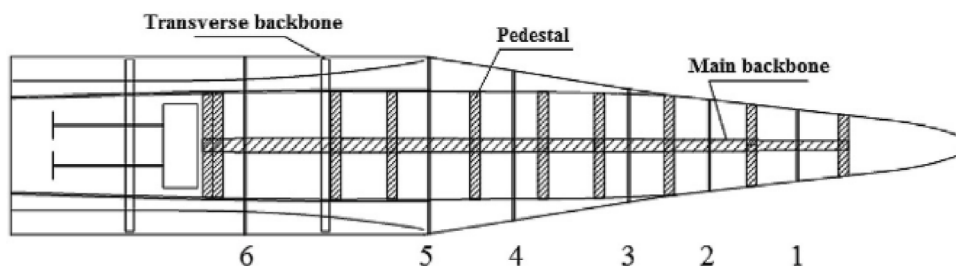
**Fig. 4.** A trimaran model featuring a longitudinal backbone and two transverse backbones [41].
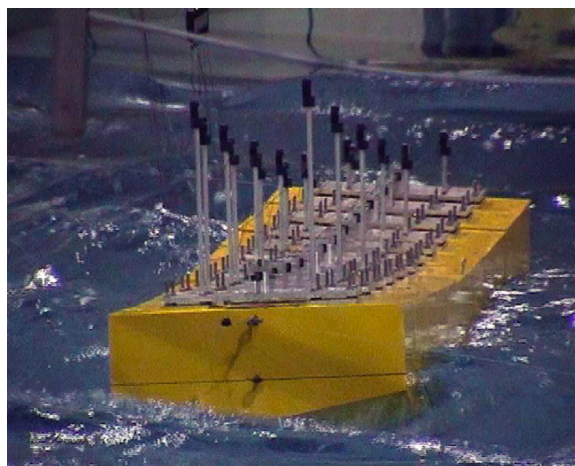


**Fig. 5.** A clear demonstration of the large responses in waves of the flexible barge used in the benchmark study [45].

longitudinally for the vertical bending of the main hull, and two transverse backbones were used to connect the side hulls (Fig. 4). The 2-node vertical bending natural frequency was scaled accurately, but there is no indication about the accuracy of horizontal bending and/or torsional scaling. The experimental measurements agreed relatively well with numerical predictions [41].

### 4.2. Benchmarking studies and technique variations

Many researchers investigate either improving methods to obtain hydroelastic data or perform experiments that are designed to be used as benchmarks. Design of flexible models was extensively discussed by Wu et al. [7], who investigated the ways in which it can be optimised by selecting, for example, the ideal number of segments for the investigation. Marón & Kapsenberg [43] analysed the various aspects of the design process of a hydroelastic model and classified the options a researcher is called to choose from. They argued that hammer tests for the determination of dry modes are insufficient because of the significant amount of noise in the responses and the first mode masking the rest; testing with shakers which apply loads at specific frequencies was suggested instead. The publication focused on the ways to organise the design, construction and experimentation process to achieve accurate results.

Ramos et al. modified a model of the S175 container ship previously used by the International Towing Tank Conference (ITTC) for seakeeping experiments to perform hydroelastic testing [44]. They cut the model in 4 segments and introduced flexible bars between each pair of segments. Both bending moments and shear stresses were measured in each of the segments. Their measurements were compared to predictions from analytical formulas with relatively good agreement.

Malenica et al. constructed a simplified model of a rectangular barge as part of a benchmark study [29]. The barge did not represent a real vessel but was designed to be very flexible, to the point that its deformations were clearly visible with the naked eye and could be monitored by optical systems (Fig. 5). The barge was subsequently subjected to waves in various headings and the RAOs in vertical bending [29], horizontal bending and torsion [46] were measured. The results were used to validate numerical codes, which were found to agree well.

Lavroff et al. manufactured a 2-segment model of a slender hull to investigate the effects of stiffness and mass distribution on the natural frequencies [47]. Interestingly, each of the segments featured an aluminium backbone at the level of the main deck, and the two backbones were connected at the amidships cut with a torsional spring. The fibreglass hull segments and the aluminium backbones had a degree of flexibility, and various levels of stiffness for the torsional spring were tested. Modal tests were performed in water with varying amidships stiffness and longitudinal mass distribution.
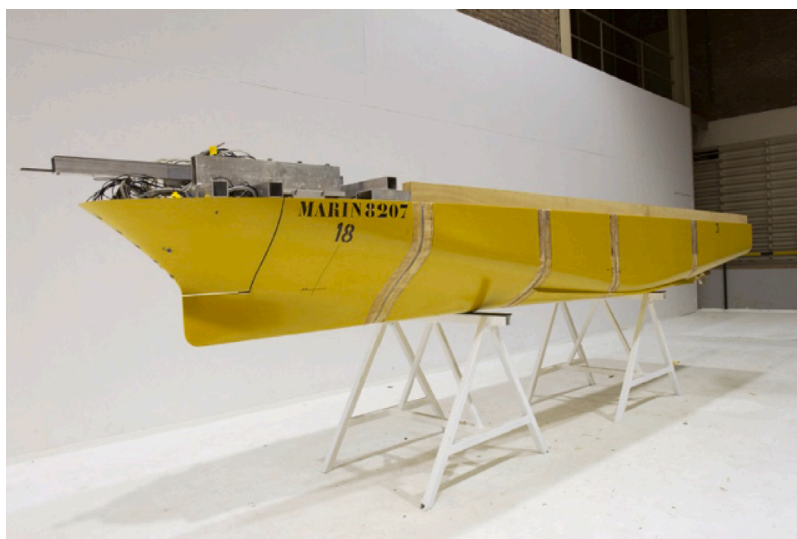
**Fig. 6.** Drummen & Holtmann introduced the upper bow of a Ro-Ro as a pseudo-segment to measure slamming loads [53].

Coppotelli et al. used a flexible backbone model to investigate an output-only analysis, suggesting their methodology for the identification of modal parameters of full scale ships at sea, where wave excitation is not measurable [48]. It was demonstrated that, using this method, it is possible to retrieve significant amount of information concerning the ship structure itself [49]. The technique was validated by comparison of model test results and full-scale measurements [50].

Adenya et al. used a flexible backbone model of an ore carrier to investigate springing responses [51]. They used two different backbones, both of variable stiffness distribution, to identify the effects of increased flexibility to the responses of the vessel. They found that the rigid body responses were not affected by the degree of flexibility, and their hydroelastic predictions agreed well with experimental measurements. The importance of the use of the convoluted backbone system, which near the ends of the vessel used a single backbone and in the area of the parallel middle body used a double backbone, was not fully explained.

Chen et al. created two almost identical backbone models of a 15,000 TEU container ship to investigate the effects of self-propulsion of the model, as opposed to towing it [52]. The towed model had 10 segments and the self-propelled model had 6 segments, as the aft part containing the motors and shafts had to be rigid. For both models a system of steel backbones, similar to [51] was used. The individual backbones were of variable rectangular cross section, and both springing and whipping responses were measured. The natural frequency of the self-propelled model was found to be 27% lower than that of the towed model. As would be expected, the model with more segments could emulate more mode shapes accurately. The propulsion system was also found to have significant effects on the high-frequency content of the response.

Drummen & Holtmann coordinated a benchmark study, for which the experiments were performed in Maritime Research Institute Netherlands (MARIN) using a flexible backbone model of a Ro-Ro vessel [53]. The hull was split in 5 segments, but the upper part of the bow was separated as an additional pseudo-segment (Fig. 6). It was (rigidly) connected with force transducers to the remaining model, allowing measurement of slamming loads. Pressure gauges was also installed to measure the pressure distribution and local vibrations were measured with a series of accelerometers. The deviations between predictions of vertical force among partners were significant.

Three phases of the WILS (Wave-induced Loads on Ships) joint-industry project, initiated by the Korea Research Institute of Ships and Ocean engineering (KRISO), have been performed to benchmark predictions for loads on large container ships. In all three cases model tests were performed and compared to predictions from numerical codes of the various partners. In WILS JIP-I, the model consisted of four segments, which were linked using force transducers, with a resulting natural frequency of the correct order of magnitude. The procedure was enhanced in WILS JIP-II, where a 6-segment model with a steel backbone with a U-shaped cross section was used. The 2-node bending natural frequency of the ship was achieved with reasonably good accuracy (approximately 6% difference), whereas the error rose to 66% for the 1-node torsional mode. For both models, the nonlinear wave loads were measured. Lee et al. used the experimental measurements from WILS JIP-II to validate their springing and whipping predictions produced using a time-domain code [54,55], finding good agreement.

WILS JIP-III used the hull form from the previous phase of the project but a second backbone was also used, namely one with an H-shaped cross section to eliminate antisymmetric coupling [56]. It was demonstrated that, unlike bending moments, there is no singular way to convert measured strain to torsional moment, as the value of the shear strain also depends on the loading condition of the neighbouring areas, due to warping effects. A method to convert shear strain measurements to torsional moments was suggested, and it was demonstrated that the antisymmetric coupling can significantly affect the amplitude of the latter [57]. The springing measurements were compared to computational predictions [58].

This phase of the project (WILS JIP-III), however, focused more on the evaluation of slamming and whipping loads, and also included wedge drop tests [59]. The drop tests were used, among others, to determine the location of pressure sensors on the bow of the model. Tests in regular head and oblique waves around the ship–wave matching region produced violent slamming events, in some cases causing full submergence of the bow. Correlation between impact force and instantaneous surge velocity was found. It was also demonstrated that the forward speed of the ship and wave height are two of the governing factors for slam amplitude [60]. Correlation was also found between the amplitudes of impact load and structural responses, although clear separation between springing and whipping responses proved challenging [61]. Similar stern slamming loads were observed for head and following seas, although slam-induced whipping responses were mainly observed in following seas [62]. Significant higher-order springing responses were measured, but the harmonic part was found to dominate the response [63].

Yang et al. introduced what they called the "combined backbone" where a large backbone, almost the size of the hull, is used, and is bolted directly onto the rigid segments, rather than linked with rods [64]. The benefit of such a design is an improved approximation of the symmetric and antisymmetric natural frequencies of the vessel concurrently. The authors identified the importance of the transverse bulkhead stiffness for the appropriate scaling of the antisymmetric natural frequencies.

A relatively recent trend in measurement of ship dynamic structural response has been the so-called *large-scale models*. The distinctive characteristic of this type of testing apart from, as the name implies, the fact that the models are larger, is that they are usually tested in the sea or a lake rather than in an experimental facility. This approach has been used for a long time in other types of investigations, such as resistance or manoeuvrability, but its application in hydroelasticity is only now growing [3]. Benefits of their use for hydroelastic testing include more realistic seaways, inclusion of wave and wind loading on the hull and superstructures, and measurement of highly nonlinear fluid–structure interaction, which can be difficult to reproduce in a laboratory [3]. Their main disadvantage is that, being a larger version of a segmented model, the associated manufacturing cost is even higher, and the logistics of the testing are also significant. Furthermore, there is an inherent unpredictability of weather conditions and an area-related dependency of expected wave heights. In order to achieve appropriate wave scaling, coastal areas are usually favoured [3].

In terms of model design and manufacturing, the techniques are similar to the ones used for towing tank models. Segmented models, usually featuring a flexible backbone, are popular [65–68] although elastic models have been proposed too [3]. The main benefit of using larger models, in this case, is that it is easier to achieve scaling of the plate thickness. However, the elastic model proposed was still relatively simplified, consisting of an external shell, some longitudinal stiffeners, transverse bulkheads and decks near the ends, but missing the cellular representation of a container ship structure. Scaling of the 3-node vertical bending natural frequency was achieved with 20% error.

Lu et al. also manufactured a large-scale model of container ship, with a length of 8.157 m [69]. In this case, however, the model was not tested in open sea but in a large ocean basin. This option seems to be a good intermediate solution, as it combines reduced scaling effects with the controlled environment of a testing facility. The testing was part of a large international JIP coordinated by the China Ship Scientific Research Center (CSSRC) to assess the hydroelastic behaviour of ultra-large container ships (in this case 20,000 TEU). Some preliminary results from hydroelastic testing have already been published at the time of writing, demonstrating good agreement between experimental measurements and computational predictions for linear springing responses [70]. Furthermore, a very detailed uncertainty analysis was performed, demonstrating that the largest uncertainty was related to the sensor calibration [71].

*4.3. Hydroelastic models for investigation of slamming and whipping*

Transient hull responses due to slamming have been investigated by many researchers, focusing mainly on high-speed craft, where these responses are more common. McTaggart et al. produced a segmented model of a frigate to investigate slamming responses [72]. Their model had 6 segments and a uniform backbone consisting of a polycarbonate box section reinforced with carbon–epoxy stiffeners. Solid hardwood bulkheads were fitted inside the backbone at the segment-mounting locations. The only longitudinally continuous structural members were the carbon–epoxy stiffeners, and the purpose of the polycarbonate frame was to provide the appropriate shear stiffness. The resulting backbone emulated the scaled, vertical and horizontal, bending and shear properties of the frigate. The model was tested in severe head seas and an increase of the non-dimensionalised vertical bending moment was observed for higher wave steepness.

Hermundstad & Moan used a segmented model of a Ro-Ro vessel to evaluate the slamming responses in various wave headings (head, quartering, following) and compare that to numerical predictions [73]. The model included a cut amidships and a cut aft of the bow. The segments were connected using force transducers, scaling the 2-node bending natural frequency. Pressure panel gauges were mounted on the bow to measure average slamming pressure in those regions. During the experiments, slamming was only observed for head and quartering seas, and only during heave or pitch resonance. The measured pressure was decomposed into its hydrostatic and added mass components.

Extensive research has been performed concerning the slamming loads and whipping responses of the 112 m INCAT wave-piercing catamaran (Fig. 7). Lavroff et al. [16] used a flexible joint model featuring a separated centrebow to investigate the effect of displacement variations and forward speed on whipping. The bending loads at two cross sections along the demihulls were derived from torsional spring measurements. The dry and wet modal characteristics of the vessel were measured and used to evaluate slamming events. The damping ratio was found to significantly increase with forward speed [16]. On the other hand, slamming loads decreased with increasing wave height, due to increased immersion of the centrebow and the relevant added mass [75]. Good agreement was found between model-scale results and full-scale measurements [76]. The effect of the centrebow on ship motions
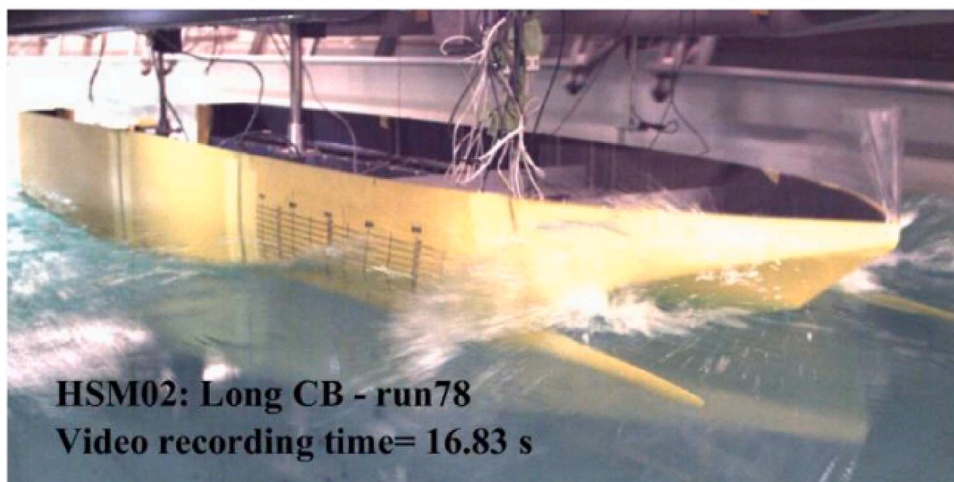
**Fig. 7.** A flexible joint model of the INCAT catamaran during centre bow slamming [74].
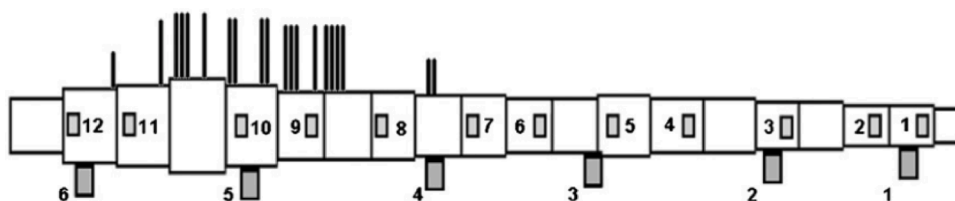


**Fig. 8.** This flexible backbone featured 20 different sections for the variation of vertical bending stiffness [86].

was investigated in more detail by Matsubara et al. [77]. The centrebow was connected to transverse beams equipped with strain gauges to evaluate slamming events.

The same model was later used to investigate extreme slam events [78] and also to determine the relationship between wave characteristics and resulting slamming [79]. The majority of slams were found to occur near the aft end of the centrebow and the general trend identified was that slam load increases with vertical velocity. However, the range of magnitudes observed for the same vertical velocity was not insignificant. Weak correlation was found between the combination of wave height and wave encounter frequency and the position of peak sagging slam load.

The lessons learned from the above studies and their predecessors were summarised by Thomas et al. in the form of guidelines [80]. The influence of wave height was investigated in more detail and results indicated strong correlation with slam load magnitude [81]. Using the same model, French et al. [82] investigated slamming in a range of irregular seas. It was demonstrated that relative vertical velocity between the ship and the free surface is not sufficient as an indicator for the resulting slamming loads. The effect of ship motion on slam loading was found to be less significant with increasing encounter frequency. The model was tested in random head seas to develop a database that can be used to predict slam occurrences [83].

The model was subsequently modified by replacing the centre bow with several alternative versions [84]. These included variation of the length of the centre bow and the height of the wet deck. It was found that slamming force increases with centre bow length and decreases with wet deck height. The slam loads and pressures were also measured in irregular seas [74].

Although the model used in the above experiments offered important insight on the mechanisms related to slamming of high-speed craft, responses could be obtained in limited detail. The joint stiffness ensured an accurate scaling of the first vertical bending natural frequency and the three segments a satisfactory representation of the relevant mode. However, the loads were only measured in two sections, and the extent to which the centre-bow deformation can be considered realistic was not demonstrated. Assuming the latter does not affect the flow around the vessel significantly, the measurements can provide insight regarding responses dominated by 2-node bending.

Ge et al. [85] compared the slamming behaviour of a catamaran, as observed in experiments, with predictions of a three-body theoretical dynamic model. A very interesting aspect of this investigation is the extensive error analysis of both the theoretical model and the experimental procedure, including consideration of wave frequency effects and seiching phenomena in the towing tank.

Very detailed work concerning a semi-displacement fast ferry (Fincantieri MDV3000) was presented by Ciappi et al. [15] who investigated both the RAOs of the vessel and its slamming behaviour. Prior to that, the model had been successfully validated using full-scale measurements [87]. The effect of forward speed on hull vibrations was investigated [33] and hydrodynamic damping was found to increase with forward speed (as in [16]), especially after the critical value for the Froude number corresponding to transom
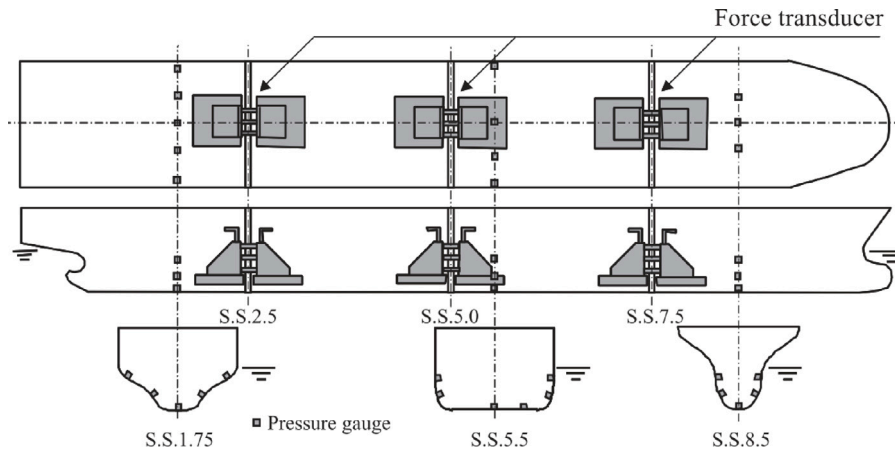
**Fig. 9.** Flexible joint model [22].



**Fig. 10.** Openings are often cut into backbones to generate antisymmetric coupling [31].

flow separation. Due to the behaviour of such monohulls, the research mainly focused on transient responses and structural loads caused by whipping. Numerical schemes were implemented to predict slamming behaviour and were compared to the experimental measurements with good agreement, especially when compared to results by Wagner and von Karman solutions [88]. Slamming was found to occur in clusters [86] where individual slamming events are mutually dependent and thus difficult to predict with statistical models. A criterion for the identification of slamming events based on measurement of whipping was proposed [89].

The backbone model of the MDV3000 featured a variable stiffness distribution, ensuring a more accurate depiction of the bending natural frequencies and modes (Fig. 8). Use of six segments longitudinally resulted in satisfactory results for the 2-node, 3-node and 4-node natural modes in vertical bending. It was demonstrated that the rubber strips commonly added between the segments to make the hull waterproof significantly increase modal damping [15]. Although this could be a good intermediate solution (in terms of structural detail) between a standard backbone model and an elastic model, the associated manufacturing complexity and cost would be more similar to the latter than the former.

Li et al. also opted for a non-uniform backbone to investigate stern slamming of large cruise ships [90]. The backbone of the 7-segment model was less complex than the one used for the Fincantieri MDV3000, but still featured 6 different sections. The first two symmetric natural frequencies were scaled with good accuracy. Significant stern slamming was observed in both head and followings seas, although its duration was shorter in following seas due to the smaller longitudinal deadrise angle in that direction.

### 4.4. Hydroelastic models for investigation of antisymmetric vibrations

The term "antisymmetric" regards hull vibrations outside the symmetry plane defined by the longitudinal and the vertical axis of the ship, namely horizontal bending and torsion. These responses are of special interest in the case of ships with large deck openings, such as container ships. The geometry of the cross sections of these ships results in a shear centre well below the level of the keel, causing strong coupling of the aforementioned vibrations.

Iijima et al. [22] compared the ability of a strip theory code and a Rankine source code to predict torsional vibration responses. A series of experiments were conducted for validation purposes, where the segments were linked by a series of force transducers (Fig. 9). The container ship model was subjected to regular waves from directions between 0° and 180° at 30° intervals. Good agreement with the experimental results was observed for the Rankine method, especially for small wave heights. Strip theory produced less satisfactory results, while both methods lacked accuracy for the extreme wave height of 15 m. The latter was attributed to nonlinearities in the bending moments near the bow section (this effect would be later investigated in greater detail by Zhu et al. [31], see 4.5). It was concluded that the worst loading condition results from waves of length equal to 35% of the ship length, approaching at a 120° angle.

A different approach was presented by Iijima et al. where the stiffness distribution was achieved by employing an aluminium backbone with openings along the length [30]. The model consisted of 17 rigid segments made of Divinycell foam and the backbone was located on the main deck (Fig. 10). The resulting bending (horizontal and vertical) and torsional natural frequencies demonstrated adequately small error after scaling. The advantages, however, of a model with a number of segments significantly greater than what is standard practice were not demonstrated. Furthermore, the correct shear centre location (below the hull) could not be achieved and, consequently, the horizontal bending and twisting modes were not coupled appropriately. An investigation of the higher-order harmonic responses followed [31] and the measurements were used to validate numerical codes [91] with good agreement. A similar model was used by Oka et al. but little information was provided concerning the design of the backbone to achieve the desired distributed stiffness and shear centre location [25].

The above experiments demonstrate the limitations of segmented models more profoundly. Symmetric vibration experiments mainly rely on the accurate scaling of the two-node vertical bending natural mode and the relevant natural frequency. When investigating antisymmetric responses, however, accurate depiction of the stiffness distribution and the location of the shear centre are crucial. As discussed in Houtani et al. [38] and Grammatikopoulos [92], the correct location of the shear centre (and, consequently, appropriate coupling of the antisymmetric modes) is, with very few exceptions, not achieved with non-elastic models. Achieving these design requirements without a continuous model results in a backbone mimicking a ship shape, which overcomplicates the design and still fails to achieve the correct level of antisymmetric coupling.

## 4.5. Hydroelastic models for experiments including nonlinear hydrodynamics

Storhaug & Moan extensively investigated the effect of the geometry of the moving ship on the waves encountered [93]. A series of hypotheses concerning the interactions of waves and a blunt wall in motion, such as the bow of the ship, were modelled numerically. Experimental implications were addressed, including the inability to produce, in a towing tank, waves corresponding to an encounter frequency approximating the 2-node natural frequency of a stiff vessel unless a small scaling factor is used.

Takaoka et al. investigated the effect of stiffness distribution on the behaviour of a flexible backbone model for two container ship sizes (5000 and 13,000 TEU, respectively) [24]. Their work, concerning whipping phenomena, concluded that the percentage of increase in bending moment amidships due to whipping was not affected significantly by the stiffness distribution (uniform or variable). Contrary to their expectations, no strong correlation between ship size and slam loads was observed but it was reported that bow flare shape has a significant effect. Previous research had already established the nonlinear contributions of the latter on vertical bending moments (e.g. [94,95]). Watanabe et al. in particular, produced an elastic model for the S-175 container ship and a modified model of the same ship with increased flare [10]. Although the double amplitude of the vertical bending moment measured was not significantly different due to the bow modification, peak values of sagging bending moment were found to increase. Similarly, Zhu et al. performed tests in head, oblique and quartering seas [91] and investigated the effect of bow flare shape on torsional vibration of the hull [31]. High-frequency responses were found to be almost dominant in irregular waves with short wave peak periods, an effect which seemed to increase with forward speed [96].

Nonlinearities in wave-induced loads were investigated, both experimentally and numerically, for large [97,98] and ultra-large [99,100] container ships. Drummen et al. measured a significant contribution of the 4th and 6th harmonic to the bending moment (up to 50% of that of the 1st harmonic) [97]. The results by Zhu & Moan agree with the above [98]; in this case, the underestimation of loads is demonstrated by experiments and calculations for a 8600-TEU container ship. Experiments for this vessel, as well as one with capacity of 13,000-TEU indicate limited asymmetry between hogging and sagging vertical bending moments, with an increase due to high-frequency vibrations being more significant in the latter [99]. This increase was found to vary with heading angle of the waves, with significant increase under 30° angle and 60° angle for hogging and sagging, respectively [100].

Miyake et al. focused on superharmonic resonance phenomena for a mega-container ship [28]. Their experimental data suggested that irregular seas result in more severe responses than similar regular waves, as the former induced direct springing of the hull. Fonseca et al. compared numerical results with experimental data and commented on the lack of accuracy of strip theory with increasing vessel forward speed [101]. Experiments using the same model (S-175 container ship with a "rigid" backbone, thus ignoring hydroelastic effects) were performed to shed light on the nonlinear parts of the response, concluding that nonlinear phenomena play an equally important part at low and high speeds [102]. Investigations on a more recent container ship design identified further uncertainties regarding the source of motion nonlinearities, especially when comparing the results of the two designs. Measurements of green water loads were also presented and analysed [103].

The behaviour of a blunt ship (similar to a bulk carrier or a tanker) was investigated by Zhu et al. [21] in extreme wave heights (four wave heights between 6 and 14 m in full scale). A large number of tests were performed in regular and irregular waves, head, beam, quartering and following seas and in an extensive range of wave heights and lengths. The model comprised of two segments connected with a force transducer and the measurements included hull and green water pressures, as well as horizontal and vertical

bending moments. The investigation focused on nonlinearities caused by the increased wave height; no asymmetry in the vertical bending moment of this ship was observed, whereas significant nonlinear effects were reported in the pressures measured. The results were used to validate a simplified prediction model, designed for use in practical ship design. It was suggested that short-term values of sea states associated with extreme wave heights and resulting in extreme structural loads should be taken into account during ship design.

Denchfield et al. investigated the hydrodynamic behaviour of a Leander-class frigate in abnormal waves and investigated the effects of forward speed [104]. Increased slamming severity was observed in the presence of rogue waves, compared to a statistically equivalent irregular sea. The experimental measurements were compared to numerical results of two models: one derived from two-dimensional strip theory and a partly-nonlinear panel-based method [105]. Subsequent measurements of global structural loads [106] indicated a significant increase in maximum bending moments in both hogging and sagging direction in the presence of abnormal waves, compared to relevant random seas. It was also concluded that bending moments under these conditions can, in some cases, exceed the design rule margins.

Similarly, Kinoshita et al. investigated the behaviour of a container ship in regular and freak waves [27]. The segmented model's stiffness originated from a hollow aluminium cylinder used as a backbone. The 10 segments of a model were not rigid but manufactured from flexible urethane foam. The authors argued that the latter enabled them to capture the flexible responses due to bottom or bow flare slamming. However, the ways in which the material and the design of the structure realistically depicted the behaviour of the full scale ship were not demonstrated.

The responses of an FPSO in abnormal waves, namely a reproduction of the New Year wave, were investigated by Clauss et al. [107]. The measurements from their 3 segment model were compared to results from a range of numerical codes. It was demonstrated that the resulting loading was within classification society rules limits; furthermore, that frequency domain analysis is capable of accurately predicting the relevant bending moments. It was argued that the main advantage of time-domain analysis is the ability to predict local loads (e.g. resulting from green water or slamming). Relevant results agreed reasonably well with the experimental data [94].

Strong correlation was identified between the position of the rogue wave with respect to the vessel (phasing) and the resulting loads. The model was subsequently upgraded by installation of force transducers at two vertical levels (main deck and bottom) to identify vertical bending loads in more detail. By comparison, frequency domain methods were again found to be sufficient to predict maximum bending loads [108].

Tang et al. tested a 6-segment model of a container ship in large waves to measure nonlinear responses [109]. The non-uniform backbone model scaled the 2-node vertical bending natural frequency, but no comments on other frequencies were included. The authors observed that heave and pitch motions remained almost linear despite the increased wave height. The vertical bending moments, however, were significantly affected by higher order harmonics.

### 4.6. Hydroelastic experiments used for structural assessment

Although most investigations focus on the elastic responses of the hull-girder, the ultimate goal of these studies is to assess the structural integrity of the vessel, both locally and globally. Loading exceeding the classification society rule predictions, especially when applied periodically or as an impact, can result in structural failure incidents, namely fatigue, buckling, and plastic collapse. Identifying stress concentration points and calculating the vessel ultimate strength are essential parts of the design process.

Fatigue caused by wave-induced vibrations was investigated using scaled models of large [110] and ultra-large container ships in head [111] and quartering seas [112]. Drummen et al. demonstrated that strip theory can over-predict fatigue damage caused by wave frequency by 15% and caused by high frequencies by 120%, resulting in an overall overestimation of approximately 50% for the midship section [110]. Storhaug et al. suggested that hull vibrations are the dominant cause of fatigue cracking, with the percentage increasing from bow to stern (65% amidships) [111]. It was also found that higher fatigue loads are induced by quartering seas than head seas and that hogging moments under these circumstances can be well above those predicted by IACS [112]. Storhaug presented a review of a series of relevant experiments [113], summarising the findings and suggesting that current guidelines leave room for improvement.

Dudson et al. performed experiments with a pentamaran container ship model, which was self-propelled using four water jets and an automated pilot [20]. The 4-segment model was tested in a variety of irregular and regular waves in an ocean basin with a forward speed of 41 knots (full scale equivalent). Forces and moments were measured in all three directions and both seakeeping and manoeuvring tests were performed. The addition of rudders improved manoeuvrability and reduced horizontal bending moment in the fore part of the vessel. Further calculations demonstrated increased fatigue damage in head and quartering head seas and a significantly reduced fatigue life due to the increased flexibility of the vessel.

## 5. Measurement and conversion techniques

Global loads on ships are mostly described in terms of bending/torsional moment at various cross sections along the length, hence treating the ship as a beam. In practice, the only way those can be measured directly in experiments is if a segmented model with flexible joints is used, and the joints installed are torsional springs. For all other cases, the most common measurement is strains, using linear or shear strain gauges. Typical measurement locations include every quarter length of the ship, and perhaps subdivisions of that. For segmented models, the measurement locations normally coincide with the changes of segment.Ultimately, one of the primary tasks to produce useful results is to perform a calibration to convert the measurements to moments.

**Table 1**

A summary of the main advantages and disadvantages of various model types in the prevalent categories of experiments.

| | Flexible joint | Flexible backbone | (Fully) elastic |
|---|---|---|---|
| Calibration | Trivial, as moments are directly measured | Easy with static tests | Challenging, dynamic tests potentially needed |
| Springing responses | Mostly first mode | More modes possible, if needed, with non-uniform backbone | Many modes accurately scaled, conversion to BM still uncertain |
| Whipping responses | Mostly first mode | More modes possible, if needed, with non-uniform backbone | Many modes accurately scaled, local response measurement also potentially possible |
| Antisymmetric responses | Normally no antisymmetric coupling | Antisymmetric coupling present but with incorrect amplitude | Easy achievement of correct antisymmetric coupling |

When using backbone models, the structure has a very clear beam-like behaviour. For symmetric responses, the backbone is calibrated statically and then the calculated coefficients are used to convert direct strains to bending moments. However, as seen in Section 4.4, this procedure becomes significantly more complicated for antisymmetric responses. In this case, not only are shear strains more difficult to measure and the corresponding strain gauges take up more channels, but also there is no unique two-way correspondence between strain and moment. This means that there are several loading configurations that could cause the same level of shear strain at a specific section, and the torsional moment should be calculated based on the loading conditions of neighbouring sections as well [57].

Elastic models can introduce further issues. If the material behaves in a different way statically and dynamically, as demonstrated by Grammatikopoulos et al. [34], the accuracy of a static calibration can be considered unreliable. Concurrently, the fact that the model is also capable of capturing local responses means that the strain measurement should be carefully decomposed to the effects of various modes. The plethora of locations where strain can be measured can also act as an issue, in the sense that these should be short-listed based on the availability of measurement channels. Use of strain-field measurement techniques, such as Digital Image Correlation (DIC) could be a way to surpass this last issue. Another option is Fibre Bragg Grating (FBG) strain gauges, as used by Houtani et al. [12], since one can connect a large series of strain gauges on a single optical fibre. Even with such measurement techniques, the need for dynamic calibration and global/local mode decomposition should be addressed.

## 6. Summary and discussion

Hydroelastic experiments have evolved greatly during the past decades. Researchers have come to investigate highly nonlinear phenomena including significant changes in the submerged geometry [98], abnormal waves [105] and higher-order resonance [97]. The measurements have been used to assess the structural integrity of the vessel and, in some cases, the responses after damage were modelled [23,26,114]. The effects of whipping [16] and torsional loads [30] have also been investigated. More detailed load measurements were, in some cases, achieved by use of elastic models [11,115]. It has been clearly demonstrated that the hydroelastic contributions to the loads are, in many cases, quite significant and should be considered in design. Furthermore, that our understanding of dynamic loading on the ship hull is still incomplete and experiments are necessary to validate the constantly improving computational models.

Table 1 summarises the main comparisons between the different model types. Flexible joint models have the advantage that the stiffness can be tuned even post-production, and that moments are measured directly if torsional springs are used. On the other hand, aspects like antisymmetric coupling or warping responses cannot be introduced. Furthermore, although in theory this concept could be used to achieve a highly variable stiffness for the hull, it has only been applied with a small number of segments (mostly 4). Consequently, what could be one of the main strengths of this type of model has not been implemented, perhaps due to cost.

As far as linear (and perhaps nonlinear) symmetric springing is concerned, segmented models with uniform backbones seem to be the best choice. These responses are mainly related to scaling of the 2-node bending natural frequency, which can be easily achieved with a uniform backbone and a minimum of 4 segments. Both the measurement with linear strain gauges and the conversion of this data to bending moments is straightforward. Using a flexible joint model or a(n) (fully) elastic model would not add any value and, in the case of the latter, would probably introduce unnecessary challenges. In this area, the way forward is probably the use of larger-scale models, either in an ocean basin or close to the shore, to reduce scaling effects.

Both whipping and antisymmetric responses appear to be more difficult to measure accurately with such models. Whipping tends to excite several flexible modes, which cannot be scaled accurately without a non-uniform stiffness distribution. This can be achieved either by using a non-uniform backbone or by manufacturing an elastic model. Antisymmetric responses are even more complicated: without the use of an elastic model, the level of antisymmetric coupling cannot be scaled appropriately. Manufacturing techniques are still the primary limiting factor in this area, with profound effects regarding the level of geometric detail that can be included and the scaling of the dynamic properties of the hull. Calibration of elastic models is another big challenge. Not only should the global and local responses be confidently separated, but also dynamic calibration might be necessary to ensure correct conversion of the strains to moments.

Looking towards the future, most changes are expected in the area of transient and antisymmetric responses. Further development of fully elastic models is needed so that the concept can mature. Strain field measuring techniques are also important to make use of the full potential of these models. Improved calibration methods, accounting for the difference between static and dynamic moduli of plastics, are also required. Models with concurrent global and local scaling would be a particularly exciting prospect.

**Table 2**

Summary of models, including the corresponding publications, number of segments and characteristics of the stiffness source for each one. The damping ratio corresponds to the first dry mode, unless it was only available for the first wet mode (specified in brackets where appropriate).

| # | Vessel type | First use | Publications | Segments | Stiffness | Structure type | Damping ($\zeta$) |
|---|---|---|---|---|---|---|---|
| 1 | Generic hull | Akita (1954) | [18,35–37] | 1 | Variable | Elastic, brass | |
| 2 | Container ship, S175 | Fukasawa (1981) | [19] | 1 | Variable | Elastic, PVC foam | 2.2% |
| 3 | Container ship, S175 | Watanabe (1989) | [10,101] | 1 | Variable | Elastic, Urethane foam | 5.1% |
| 4 | Frigate | McTaggart (1997) | [72] | 6 | Uniform | FRP backbone | 2.7% |
| 5 | Container ship, S175 | Ramos (2000) | [44] | 4 | Uniform | Flexible bars | 2.9% |
| 6 | Container ship, S175 | Chen (2001) | [9,11,115] | 1 | Variable | Elastic, ABS | 6.7% (Wet) |
| 7 | Pentamaran | Dudson (2001) | [20] | 4 | Uniform | Force transducers | |
| 8 | Blunt ship | Zhu (2002) | [21] | 2 | Uniform | Force transducers | |
| 9 | Fast ferry, MDV3000 | Ciappi (2003) | [15,33,48–50,86–89] | 6 | Variable | Aluminium backbone | 0.45% |
| 10 | Barge | Malenica (2003) | [29,46,116] | 12 | Uniform | Two steel backbones | |
| 11 | Container ship, S175 | Fonseca (2004) | [102] | 3 | Uniform | Steel backbone | |
| 12 | FPSO | Clauss (2004) | [94,107,108] | 3 | Uniform | Connecting elements | |
| 13 | Container ship, Post-Panamax | Iijima (2004) | [22] | 4 | Rigid | Force transducers | |
| 14 | Ro-Ro, Autoprestige | Hermundstad (2005) | [73] | 3 | Uniform | Force transducers | |
| 15 | Ro-Ro | Korkut (2004) | [23,117] | 2 | Rigid | Force transducers | |
| 16 | Container ship, Post-Panamax | Fonseca (2005) | [103] | 4 | Uniform | Steel backbone | |
| 17 | Catamaran | Ge (2005) | [85] | 3 | Uniform | Force transducers | |
| 18 | Container ship, Post-Panamax | Kinoshita (2006) | [27] | 10 | Uniform | Aluminium backbone | |
| 19 | Bulk carrier | Storhaug (2006) | [93] | 4 | Uniform | Flexible joints | 1.0% (Wet) |
| 20 | Slender hull | Lavroff (2006) | [47] | 2 | Variable | Torsional spring | 1.0% (Wet) |
| 21 | Catamaran, INCAT 112 m | Lavroff (2007) | [16,74–84,118,119] | 3 | Both | Torsional springs | 0.6% |
| 22 | Container ship, Post-Panamax | Drummen (2008) | [97,110] | 4 | Uniform | Torsional springs | 1.0% |
| 23 | Container ship, small | Clauss (2010) | [120] | 2 | Rigid | Torsional springs | |
| 24 | Container ship, 6500 TEU | Kim (2010) | [54–63,121] | 6 | Uniform | Steel backbone | 1.85% |
| 25 | Cruise ship | Rousset (2010) | [122] | 4 | Rigid | Aluminium–carbon backbone | |
| 26 | Frigate, Leander class | Denchfield (2010) | [17,105,106,114,123–125] | 5 | Uniform | Aluminium backbone | |
| 27 | Container ship, 12,000 TEU | Miyake (2009) | [28] | 8 | Uniform | Steel backbone | 1.0% |
| 28 | Container ship | Oka (2009) | [25] | 4 | Variable | Aluminium backbone | |
| 29 | Container ship, Post-Panamax | Iijima (2009) | [30,31,91,96,98] | 17 | Uniform | Aluminium backbone | 0.1% |
| 30 | Container ship | Storhaug (2010) | [7,98,99,111–113] | 4 | Uniform | Torsional springs | 0.9% |
| 31 | Container ship, 13,000 TEU | Storhaug (2010) | [98,99,126] | 4 | Uniform | Flexible joints | 0.9% |
| 32 | Ore carrier | Chen (2012) | [51,127] | 9 | Variable | Steel backbone | |
| 33 | Container ship, 13,000 TEU | Takaoka (2012) | [24] | 8 | Both | Two steel backbones | |
| 34 | Container ship, small | Peng (2014) | [128] | 6 | Uniform | Aluminium backbone | |
| 35 | Container ship, large | Marón (2014) | [43] | 4 | Uniform | Aluminium backbone | 2.0% |
| 36 | Ro-Ro | Drummen (2014) | [53] | 5 | Uniform | Aluminium backbone | 0.8% (Wet) |
| 37 | Barge | Iijima (2015) | [26] | 2 | Uniform | Flexible joints | |
| 38 | Container ship, large | Jiao (2015) | [65–68] | 7 | Variable | Steel backbone | |
| 39 | Trimaran | Tang (2017) | [41,42] | 7 | Variable | Steel backbones | 1.0% |
| 40 | Container ship, 6600 TEU | Houtani (2018) | [12,38] | 1 | Variable | Elastic, Urethane foam | 2.2% |
| 41 | Barge, S175 | Grammatikopoulos (2018) | [13,39,40] | 1 | Uniform | Elastic, ABS | 0.67% |
| 42 | Container ship, 20,000 TEU | Yang (2021) | [64] | 7 | Variable | Steel backbone | |
| 43 | Container ship, 10,000 | Tang (2022) | [109] | 6 | Variable | Steel backbone | |
| 44 | Container ship, 20,000 | Lu (2022) | [69–71] | 14 | Variable | Two steel backbones | 0.93% |
| 45 | Cruise ship | Li (2022) | [90] | 7 | Variable | Steel backbone | |
| 46 | Container ship, 15,000 TEU | Chen (2022) | [52] | 10 | Variable | Steel backbone | |

## Declaration of competing interest

The authors declare that they have no known competing financial interests or personal relationships that could have appeared to influence the work reported in this paper.

## Data availability

No data was used for the research described in the article.

## References

[1] Hudson DE. Scale model principles. In: Hams C, Crede C, editors. Shock and vibration handbook. New York: McGraW-Hill; 1967.

[2] Castoldi A, Casirati M. Experimental techniques for the dynamic analysis of complex structures. In: The anti-seismic design of nuclear installations. 1975, p. 326–37.

[3] Jiao J, Ren H, Guedes Soares C. A review of large-scale model at-sea measurements for ship hydrodynamics and structural loads. Ocean Eng 2021;227.

[4] Lloyd A. Seakeeping : Ship behaviour in rough weather. Gosport: A.R.J.M. Lloyd; 1998.

[5] Harris HG, Sabnis G. Structural modelling and experimental techniques. 2nd ed.. CRC Press; 1999.

[6] Bishop RED, Price WG. Hydroelasticity of ships. Cambridge University Press; 1979.

[7] Wu M, Lehn E, Moan T. Design of a segmented model for ship seakeeping tests with hydroelastic effects. In: Proceedings of the 6th international conference on hydroelasticity in marine technology. Tokyo, Japan; 2012, p. 135–44.

[8] Thomas GA, Davis MR, Holloway DS, Roberts T. The whipping vibration of large high speed catamarans. Int J Marit Eng 2003.

[9] Wu Y-S, Chen R-Z, Lin J-R. Experimental technique of hydroelastic ship model. In: Proceedings of the third international conference on hydroelasticity, Oxford, UK, September. 2003, p. 15–7.

[10] Watanabe I, Ueno M, Sawada H. Effects of Bow Flare Shape to the Wave Loads of a container ship. J Soc Nav Archit Japan 1989;1989(166):259–66.

[11] Chen R-Z, Du S-X, Wu Y-S, Lin J-R, Hu J-J, Yue Y-L. Experiment on extreme wave loads of a flexible ship model. In: Practical design of ships and other floating structures. Proceedings of the eighth international symposium on practical design of ships and other floating structures, Vol. 2. 2001, p. 871–8.

[12] Houtani H, Komoriyama Y, Matsui S, Oka M, Sawada H, Tanaka Y, Tanizawa K. Designing a hydro-structural model ship to experimentally measure its vertical-bending and torshional vibrations. J Adv Res Ocean Eng 2018;4(4):174–84.

[13] Grammatikopoulos A, Banks J, Temarel P. The design and commissioning of a fully elastic model of a uniform container ship. Mar Struct 2021;78.

[14] Ewins DJ. Modal testing: Theory, practice and application. 2000, p. 562.

[15] Ciappi E, Dessi D, Mariani R. Slamming and whipping response analysis of a fast monohull via segmented model tests. In: Proceedings of the 3rd international conference on hydroelasticity in marine technology. 2003, p. 143–55.

[16] Lavroff J, Davis MR, Holloway DS, Thomas GA. The whipping vibratory response of a hydroelastic segmented catamaran model. In: Ninth international conference on fast sea transportation. Shanhai, China; 2007.

[17] Denchfield SS, Wood C, Hudson DA, Tan M, Temarel P. Comparisons between CFD predictions and experiments for rogue wave-ship interactions. In: 11th international symposium on practical design of ships and other floating structures. Rio de Janeiro; 2010.

[18] Akita Y, Ochi K. Investigations on the strength of ships going in waves by model experiments. J Zosen Kiokai 1954;1954(97):153–9.

[19] Fukasawa T, Yamamoto Y, Fujino M, Motora S. Motion and longitudinal strength of a ship in head sea and the effects of non-linearities (4th report). J Soc Nav Archit Japan 1981;150(143):308–14.

[20] Dudson E, Rambech HJ, Wu M. Determination of wave bending loads on a 40 knot , long slender open topped containership through model tests and hydrodynamic calculations with particular reference to the effects of hull flexibility on fatigue life. In: FAST 2001 the 6th international conference on fast sea transportation, no. September. 2001.

[21] Zhu T, Kumano A, Shigemi T, Matsumani R. A consideration of wave-induced loads for direct strength calculation under extreme waves. NK Tech Bull 2002;69–80.

[22] Iijima K, Shigemi T, Miyake R, Kumano A. A practical method for torsional strength assessment of container ship structures. Mar Struct 2004;17(5):355–84.

[23] Korkut E, Atlar M, İncecik A. An experimental study of global loads acting on an intact and damaged Ro–Ro ship model, Vol. 32. 2005, p. 1370–403.

[24] Takaoka Y, Murakami A, Yoshida T, Miyake R, Yamamoto N, Terai K, Kensaku T. An Experimental Study on the whipping response of large container carriers. In: Proceedings of the 6th international conference on hydroelasticity in marine technology. Tokyo, Japan; 2012, p. 145–52.

[25] Oka M, Oka S, Ogawa Y. An experimental study on wave loads of a large container ship and its hydroelastic vibration. In: Proceedings of the 5th international conference on hydroelasticity in marine technology. 2009.

[26] Iijima K, Suzaki Y, Fujikubo M. Scaled model tests for the post-ultimate strength collapse behaviour of a ship's hull girder under whipping loads. Ships Offshore Struct 2015;10(1):31–8.

[27] Kinoshita T, Shi J-s, Nakasumi S, Kameoka H, Suzuki K, Waseda T, Tanizawa K, Yuhara T. Longitudinal loads on a container ship in extreme regular sea and freak wave. In: Proceedings of the 4th international conference on hydroelasticity in marine technology, Vol. 1. 2006, p. 103–10.

[28] Miyake R, Matsumoto T, Zhu T, Usami A, Dobashi H. Experimental studies on the hydroelastic response using a flexible Mega-Container ship model. In: Proceedings of the 5th international conference on hydroelasticity in marine technology. Southampton, United Kingdom; 2009, p. 161–71.

[29] Malenica Š, Molin B, Remy F, Senjanović I. Hydroelastic response of a barge to impulsive and non-impulsive wave loads. In: Proceedings of the 3rd international conference on hydroelasticity in marine technology. 2003.

[30] Iijima K, Hermundstad OA, Zhu S, Moan T. Symmetric and antisymmetric vibrations of a hydroelastically scaled model. In: Proceedings of the 5th international conference on hydroelasticity in marine technology, Vol. 1213796053. 2009.

[31] Zhu S, Wu M, Moan T. Experimental investigation of hull girder vibrations of a flexible backbone model in bending and torsion. Appl Ocean Res 2011;33(4):252–74.

[32] Thomas GA, Davis MR, Holloway DS, Roberts T. The vibratory damping of large high-speed catamarans. Mar Struct 2008;21(1):1–22.

[33] Dessi D, Mariani R, Coppotelli G. Experimental investigation of the bending vibrations of a fast vessel. Aust J Mech Eng 2007;4(2):125.

[34] Grammatikopoulos A, Banks J, Temarel P. Experimental dynamic properties of ABS cellular beams produced using additive manufacturing. In: ECCM18 - 18th European conference on composite materials. Athens, Greece; 2018.

[35] Akita Y, Ochi K. Investigations on the strength of ships going in waves by model experiments, (the second report): On the influence of wave length. J Zosen Kiokai 1954;95:153–9.

[36] Akita Y, Ochi K. Investigations on the strength of ships going in waves by model experiments. (the third report): On the influences of ship draughts and trims. J Zosen Kiokai 1955;97:79–86.

[37] Ochi K. Investigation on the influence of ship forms upon the strength of ships going in waves. J Zosen Kiokai 1956;100:91–9.

[38] Houtani H, Komoriyama Y, Matsui S, Oka M, Sawada H, Tanaka Y, Tanizawa K. Designing a hydro-structural model ship to experimentally measure its vertical-bending and torsional vibrations. In: 8th international conference on hydroelasticity in marine technology. Seoul, Korea; 2018.

[39] Grammatikopoulos A, Banks J, Temarel P. Prediction of the vibratory properties of ship models with realistic structural configurations produced using additive manufacturing. Mar Struct 2020;73.

[40] Grammatikopoulos A, Banks J, Temarel P. Experimental hydroelastic responses of an elastic container ship-inspired barge model produced using additive manufacturing. In: 8th international conference on hydroelasticity in marine technology. Seoul, Korea; 2018, p. 75–84.

[41] Chen Z, Gui HB, Dong P, Yu C. Numerical and experimental analysis of hydroelastic responses of a high-speed trimaran in oblique irregular waves. Int J Nav Archit Ocean Eng 2019;11(1):409–21.

[42] Tang H, Ren HL, Wan Q. Investigation of longitudinal vibrations and slamming of a trimaran in regular waves. J Ship Res 2017;61(3):153–66.

[43] Marón A, Kapsenberg GK. Design of a ship model for hydro-elastic experiments in waves. Int J Nav Archit Ocean Eng 2014;6(4):1130–47.

[44] Ramos J, İncecik A, Guedes Soares C. Experimental study of slam-induced stresses in a containership. Mar Struct 2000;13(1):25–51.

[45] Senjanović I, Malenica Š, Tomašević S. Hydroelasticity of large container ships. Mar Struct 2009;22(2):287–314.

[46] Remy F, Molin B, Ledoux A. Experimental and numerical study of the wave response of a flexible barge. In: Proceedings of the 4th international conference on hydroelasticity in marine technology. 2006.

[47] Lavroff J, Davis MR, Holloway DS, Thomas GA. Experimental analysis of the wet flexural mode response of an NPL 6A hydroelastic segmented model. In: 5th international conference on high performance marine vehicles. 2006, p. 8–10.

[48] Coppotelli G, Dessi D, Mariani R, Rimondi M. Output-only analysis for modal parameters estimation of an elastically scaled ship. J Ship Res 2008;52(1):45–56.

[49] Dessi D, Mariani R. Structure and load identification using wave excitation in seakeeping tests. In: 20th IWWWFB, Spitsbergen, Norway. 2005, p. 6–9.

[50] Dessi D, Engle A, Gu X, Ha T, Hodgson T. Impulsive pressure loading and response assessment. In: Proceedings of the 17th ship and offshore structures congress, Vol. 2. 2009, p. 367–432.

[51] Adenya CA, Ren HL, Li H, Wang D. Estimation of springing response for 550 000 DWT ore carrier. J Mar Sci Appl 2016;15(3):260–8.

[52] Chen Z, Zhao N, Zhao H, Guo R, Zhao W. Experimental parametric study on hydroelastic behaviour of a 15000-TEU container ship based on segmented ship model. Ships Offshore Struct 2022. ISSN.

[53] Drummen I, Holtmann M. Benchmark study of slamming and whipping. Ocean Eng 2014;86:3–10.

[54] Lee Y, Wang Z, White N, Hirdaris SE. Time domain analysis of springing and whipping responses acting on a large container ship. In: Proceedings of the ASME 2011 30th international conference on ocean, offshore and arctic engineering OMAE2011. Rotterdam, The Netherlands; 2011, p. 1–9.

[55] Lee YW, White N, Wang Z, Zhang S, Hirdaris SE. Comparison of springing and whipping responses of model tests with predicted nonlinear hydroelastic analyses. Int J Offshore Polar Eng 2012;22(3):1–8.

[56] Hong SY, Kim BW, Nam BW. Experimental study on torsion springing and whipping of a large container ship. In: Proceedings of the twenty-ffirst (2011) international ocean and polar engineering conference. 2011, p. 486–94.

[57] Kim BW, Kim K-H, Kim YS, Hong SY. Torsion moment conversion methods in model test with U-shape backbone. In: Proceedings of the twenty-fourth (2014) international ocean and polar engineering conference. 2014, p. 782–91.

[58] Kim JH, Kim Y, Kang BC, Kim Y. Ship springing analysis for very large container ship. Int J Offshore Polar Eng 2012;22(3):217–24.

[59] Kim JH, Kim Y, Korobkin A. Comparison of fully coupled hydroelastic computation and segmented model test results for slamming and whipping loads. Int J Nav Archit Ocean Eng 2014;6(4):1064–81.

[60] Hong SY, Kim KH, Kim BW, Kim YS. Experimental study on the bow-flare slamming of a 10,000 teu containership. In: The twenty-fourth international ocean and polar engineering conference. 2014.

[61] Hong SY, Kim K-H, Wan Kim B, Kim Y-S. Characteristics of bow-flare slamming loads on an ultra-large containership in irregular waves. In: The twenty-fifth international offshore and polar engineering conference. 2015, p. 75–81.

[62] Kim K-H, Kim BW, Hong SY, Kim Y-S. Characteristics of stern slamming loads on an ultra-large containership in irregular waves. In: The twenty-fifth international offshore and polar engineering conference. International Society of Offshore and Polar Engineers; 2015, p. 89–95.

[63] Hong SY, Kim BW. Experimental investigations of higher-order springing and whipping-WILS project. Int J Nav Archit Ocean Eng 2014;6(4):1160–81.

[64] Yang P, Feng Q, Chen H, Wen L. Combined backbone application on numerical simulations and a model experiment of a 20,000 TEU container ship. Ocean Eng 2021;223.

[65] Jiao JL, Ren HL, Adenya CA. Experimental and numerical analysis of hull girder vibrations and bow impact of a large ship sailing in waves. Shock Vib 2015;2015.

[66] Jiao JL, Ren HL, Sun SZ, Li X, Wang ZY. Measurement technique of ship hydrodynamic experiments by large-scale free running model sea trial. In: Proceedings of the international offshore and polar engineering conference, Vol. 2016-Janua. 2016, p. 737–43.

[67] Jiao JL, Ren HL. Characteristics of bow-flare slamming and hydroelastic vibrations of a vessel in severe irregular waves investigated by segmented model experiments. J Vibroeng 2016;18(4):2475–94.

[68] Jiao JL, Ren HL, zheng Sun S, Adenya CA. Investigation of a ship's hydroelasticity and seakeeping performance by means of large-scale segmented self-propelling model sea trials. J Zhejiang Univ-Sci A 2016;17(6):468.

[69] Lu Y, Liu J, Teng B, Tian C, Si H, Zhou Q, Ni X. Modal investigation on a large-scale containership model for hydroelastic analysis. Shock Vib 2022;2022.

[70] Lu Y, Liu J, Teng B, Tian C, Si H, Ni X. Linear springing assessment of ultra large container ships. In: Proceedings of the thirty-second (2022) international ocean and polar engineering conference. 2022, p. 2353–60.

[71] Si H, Yang P, Gu X, Hu J, Tian C, Feng Q, Ni Y. Uncertainty analysis of linear vertical bending moment in model tests and numerical prediction. Mech Syst Signal Process 2022;178:109331.

[72] McTaggart K, Datta I, Stirling A, Gibson S, Glen I, Brown JC, Dalzell JF, Engle A, Magee A. Motions and loads of a hydroelastic frigate model in severe seas. Trans - Soc Nav Archit Mar Eng 1997;105:427–53.

[73] Hermundstad OA, Moan T. Numerical and experimental analysis of bow flare slamming on a Ro-Ro vessel in regular oblique waves. J Mar Sci Technol 2005;10(3):105–22.

[74] Shabani B, Lavroff J, Davis MR, Holloway DS, Thomas GA. Slam loads and pressures acting on high-speed wave-piercing catamarans in regular waves. Mar Struct 2019;66:136–53.

[75] Lavroff J, Davis MR, Holloway DS, Thomas GA. The vibratory response of high-speed catamarans to slamming investigated by hydroelastic segmented model experiments. Int J Marit Eng 2009;151(4):1–13.

[76] Davis MR, Thomas GA, Holloway DS, Lavroff J, Amin W, Matsubara S, Roberts T. Slamming and whipping of wave-piercing catamarans. In: Proceedings of the 5th international conference on hydroelasticity in marine technology. Southampton, United Kingdom; 2009, p. 223–32.

[77] Matsubara S, Thomas GA, Davis MR, Holloway DS, Roberts T. Influence of centrebow on motions and loads of high-speed catamarans. In: FAST 2011 11th international conference on fast sea transportation, no. September. 2011, p. 661–8.

[78] Thomas GA, Winkler S, Davis MR, Holloway DS, Matsubara S, Lavroff J, French BJ. Slam events of high-speed catamarans in irregular waves. J Mar Sci Technol 2011;16(1):8–21.

[79] Lavroff J, Davis MR, Holloway DS, Thomas GA. Determination of wave slamming loads on high-speed catamarans by hydroelastic segmented model experiments. Int J Marit Eng 2011;153(A3):185–97.

[80] Thomas GA, Matsubara S, Davis MR, French BJ, Lavroff J, Amin W. Lessons learnt through the design, construction and testing of a hydroelastic model for determining motions, loads and slamming behavior in severe sea states. In: Proceedings of the 6th international conference on hydroelasticity in marine technology. Tokyo, Japan; 2012, p. 163–72.

[81] Lavroff J, Davis MR, Holloway DS, Thomas GA. Wave slamming loads on wave-piercer catamarans operating at high-speed determined by hydro-elastic segmented model experiments. Mar Struct 2013;33:120–42.

[82] French BJ, Thomas GA, Davis MR. Slam characteristics of a high-speed wave piercing catamaran in irregular waves. R Inst Nav Archit Trans A 2014;156(Part A1):A25–36.

[83] Davis MR, French BJ, Thomas GA. Wave slam on wave piercing catamarans in random head seas. Ocean Eng 2017;135(November 2016):84–97.

[84] Shabani B, Lavroff J, Holloway DS, Davis MR, Thomas GA. The effect of centre bow and wet-deck geometry on wet-deck slamming loads and vertical bending moments of wave-piercing catamarans. Ocean Eng 2018;169:401–17.

[85] Ge C, Faltinsen OM, Moan T. Global hydroelastic response of catamarans due to wetdeck slamming. J Ship Res 2005;49(1):24–42.

[86] Dessi D, Ciappi E. Slamming clustering on fast ships: From impact dynamics to global response analysis. Ocean Eng 2013;62:110–22.

[87] Cusano G, Monti S, Velasco A. Full scale and model test investigation of slamming effects on fast monohull vessels. In: Proceedings of the 3rd international conference on hydroelasticity in marine technology. 2003, p. 163–73.

[88] Dessi D, Mariani R. Analysis and prediction of slamming-induced loads of a high-speed monohull in regular waves. J Ship Res 2008;52(1):71–86.

[89] Dessi D. Whipping-based criterion for the identification of slamming events. Int J Nav Archit Ocean Eng 2014;6(4):1082–95.

[90] Li H, Zou J, Deng B, Liu R, Sun S. Experimental study of stern slamming and global response of a large cruise ship in regular waves. Mar Struct 2022;86(August):103294.

[91] Zhu S, Wu M, Moan T. Experimental and numerical study of wave-induced load effects of open ships in oblique seas. J Ship Res 2011;55(2):100–23.

[92] Grammatikopoulos A. The effects of geometric detail on the vibratory responses of complex ship-like thin-walled structures. Mar Struct 2021;(78).

[93] Storhaug G, Moan T. Springing/whipping response of a large ocean-going vessel investigated by an experimental method. In: Proceedings of the 4th international conference on hydroelasticity in marine technology, Vol. 1. ASME; 2006, p. 89–102.

[94] Guedes Soares C, Fonseca N, Pascoal R, Clauss G, Schmittner CE, Hennig J. Analysis of wave induced loads on a FPSO due to abnormal waves. In: Proceedings of OMAE specialty conference on integrity of floating production, storage & offloading (FPSO) systems August 30 - September 2, 2004, Houston, TX. 2004, p. 1–8.

[95] Storhaug G, Moe E, Holtsmark G. Measurements of wave induced hull girder vibrations of an ore carrier in different trades. J Offshore Mech Arct Eng 2007;129(4):279.

[96] Zhu S, Moan T. A comparative study of the influence of bow shape on hull girder vibrations through two backbone models. In: Proceedings of the 6th international conference on hydroelasticity in marine technology, no. 1251. Tokyo, Japan; 2012, p. 153–62.

[97] Drummen I, Wu M, Moan T. Experimental and numerical study of containership responses in severe head seas. Mar Struct 2009;22(2):172–93.

[98] Zhu S, Moan T. Investigation into the nonlinear hydroelastic response of an 8600-TEU containership model advancing in regular waves. Ships Offshore Struct 2014;9(1):74–87.

[99] Zhu S, Moan T. New insight into the wave-induced nonlinear vertical load effects of ultra-large container ships based on experiments. J Mar Sci Technol 2013;18(1):87–114.

[100] Zhu S, Moan T. Nonlinear effects from wave-induced maximum vertical bending moment on a flexible ultra-large containership model in severe head and oblique seas. Mar Struct 2014;35:1–25.

[101] Fonseca N, Guedes Soares C. Comparison of numerical and experimental results of nonlinear wave-induced vertical ship motions and loads. J Mar Sci Technol 2002;6(4):193–204.

[102] Fonseca N, Guedes Soares C. Experimental investigation of the nonlinear effects on the vertical motions and loads of a containership in regular waves. J Ship Res 2004;48(2):118–47.

[103] Fonseca N, Guedes Soares C. Experimental investigation of the shipping of water on the bow of a containership. J Offshore Mech Arct Eng 2005;127(4):322.

[104] Denchfield SS, Hudson DA, Temarel P, Bateman W, Hirdaris SE. Evaluation of rogue wave induced loads using 2D hydroelasticity analysis. In: Proceedings of the 5th international conference on hydroelasticity in marine technology. Southampton, United Kingdom: University of Southampton; 2009.

[105] Bennett SS, Hudson DA, Temarel P. The influence of forward speed on ship motions in abnormal waves: Experimental measurements and numerical predictions. J Fluids Struct 2013;39:154–72.

[106] Bennett SS, Hudson DA, Temarel P. Global wave-induced loads in abnormal waves: Comparison between experimental results and classification society rules. J Fluids Struct 2014;49:498–515.

[107] Clauss G, Schmittner CE, Hennig J, Guedes Soares C, Fonseca N, Pascoal R. Bending moments of an FPSO in rogue waves. In: Proceeding of the 23rd international conference on offshore mechanics and arctic engineering (OMAE 2004). 2004, p. 1–8.

[108] Clauss G, Kauffeldt A, Jacobsen K. Longitudinal forces and bending moments of a FPSO. In: Proceeding of the 26rd international conference on offshore mechanics and arctic engineering (OMAE 2007). 2007, p. 1–10.

[109] Tang Y, Sun SL, Yang RS, Ren HL, Zhao X, Jiao JL. Nonlinear bending moments of an ultra large container ship in extreme waves based on a segmented model test. Ocean Eng 2022;243:110335.

[110] Drummen I, Storhaug G, Moan T. Experimental and numerical investigation of fatigue damage due to wave-induced vibrations in a containership in head seas. J Mar Sci Technol 2008;13(4):428–45.

[111] Storhaug G, Malenica Š, Choi B-K, Zhu S, Hermundstad OA. Consequence of whipping and springing on fatigue and extreme loading for a 13000TEU container vessel based on model tests. In: 11th international symposium on practical design of ships and other floating structures. Rio de Janeiro; 2010, p. 1201–9.

[112] Storhaug G, Derbanne Q, Choi B-K, Moan T, Hermundstad OA. Effect of whipping on fatigue and extreme loading of a 13000teu container vessel in bow quartering seas based on model tests. In: Proceedings of the 30th international conference on ocean, offshore and arctic engineering. Rotterdam, The Netherlands; 2011, p. 1–10.

[113] Storhaug G. The measured contribution of whipping and springing on the fatigue and extreme loading of container vessels. Int J Nav Archit Ocean Eng 2014;6:1096–110.

[114] Bennett SS, Phillips AB. Experimental investigation of the influence of hull damage on ship responses in waves. In: Analysis and design of marine structures V. CRC Press; 2015, p. 3.

[115] Du S-X, Hudson DA, Price WG, Temarel P, Chen R-Z, Wu Y-S. Wavelet analysis of loads on a flexible ship model traveling in large-amplitude waves. J Ship Res 2008;52(4):249–62.

[116] Senjanović I, Malenica Š, Tomašević S. Investigation of ship hydroelasticity. Ocean Eng 2008;35(5–6):523–35.

[117] Korkut E, Atlar M, İncecik A. An experimental study of motion behaviour with an intact and damaged Ro-Ro ship model. Ocean Eng 2004;31(3–4):483–512.

[118] French BJ, Thomas GA, Davis MR. Slam occurrences and loads of a high-speed wave piercer catamaran in irregular seas. Proc Inst Mech Eng M 2013;229(1):45–57.

[119] Jacobi G, Thomas GA, Davis MR, Davidson G. An insight into the slamming behaviour of large high-speed catamarans through full-scale measurements. J Mar Sci Technol 2014;19(1):15–32.

[120] Clauss G, Klein M, Dudek M. Influence of the bow shape on loads in high and steep waves. In: Proceedings of the 29th international conference on ocean, offshore and arctic engineering. 2010, p. 1–12.

[121] Kim SP, Yu H-C, Hong SY. Segmented model testing and numerical analysis of wave-induced extreme and springing loads on large container carriers. In: The twentieth international offshore and polar engineering conference. International Society of Offshore and Polar Engineers; 2010.

[122] Rousset J, Ferrant P, Alessandrini B. Experiments on a segmented ship model in directional irregular waves. In: Proceedings of the 21th international workshop on water waves and floating bodies. 2010, p. 3–6.

[123] Denchfield SS. An investigation into the influence of rogue waves on a traveling ship (Ph.D. thesis), Faculty of Engineering, Science and Mathematics School of Engineering Sciences; 2011.

[124] Denchfield SS, Winden B, Brooks C, Turnock S, Hudson DA, Forrester A, Taunton D. Wireless sensor network for determining boat motions and hydroelastic responses. Adv Meas Technol 2011;1–14.

[125] Bennett SS, Brooks C, Winden B, Taunton D, Forrester A, Turnock S, Hudson DA. Measurement of ship hydroelastic response using multiple wireless sensor nodes. Ocean Eng 2014;79:67–80.

[126] Storhaug G. Consequence of whipping and springing on fatigue for a 8600TEU container vessel in different trades based on model tests. In: 11th international symposium on practical design of ships and other floating structures, Rio de Janeiro, Brazil, 2010. 2010, p. 1180–9.

[127] Chen Z, Ren H, Li H, Zhang K. Experimental and numerical analysis of bow slamming and whipping in different sea states. J Ship Mech 2012;16(3):246–53.

[128] Peng S, Temarel P, Bennett SS, Wu W, Liu Z, Wang Y. Symmetric response of a hydroelastic scaled container ship in regular and irregular waves. In: Proceedings of the ASME 2014 33rd international conference on ocean, offshore and arctic engineering OMAE2014. San Francisco, California, USA: ASME; 2014, p. 1–10.